Untying relaxed circular DNA of hepatitis B virus by polymerase reaction provides a new option for accurate quantification and visualization of covalently closed circular DNA

Naohiro Kamiya[1,2], Takahiko Sugimoto[1], Hiromi Abe-Chayama[2,3], Rie Akiyama[2,3], Yasunori Tsuboi[1], Akira Mogami[1], Michio Imamura[2,3], C. Nelson Hayes[2,3], Kazuaki Chayama[2,3,4,*]

[1] Research Unit/Immunology & Inflammation, Sohyaku, Innovative Research Division, Mitsubishi Tanabe Pharma Corporation, Yokohama, Kanagawa, Japan

[2] Department of Gastroenterology and Metabolism, Graduate School of Biomedical and Health Sciences, Hiroshima University, Hiroshima, Hiroshima, Japan

[3]Research Center for Hepatology and Gastroenterology, Hiroshima University, Hiroshima, Japan.

[4]Institute of Physical and Chemical Research (RIKEN) Center for Integrative Medical Sciences, Yokohama, Japan.

[*] Corresponding author: chayama@hiroshima-u.ac.jp (KC)

Kazuaki Chayama, MD, PhD, Department of Gastroenterology and Metabolism, Applied Life Sciences, Institute of Biomedical & Health Sciences, Hiroshima University, 1-2-3 Kasumi, Minami-ku, Hiroshima 734-8551, Japan. Telephone: +81-82-257-5192, Fax: +81-82-257-5194

(From 2021 Apr) Collaborative Research Laboratory of Medical Innovation, Hiroshima University

Abstract

Hepatitis B virus (HBV) is a small hepatotropic DNA virus that replicates via an RNA intermediate. After entry, the virus capsid carries relaxed circular DNA (rcDNA) into the nucleus where the viral genome is converted into covalently closed circular DNA (cccDNA), which serves as the template for all viral transcripts. To monitor cccDNA levels, preprocessing methods to eliminate rcDNA have emerged for quantitative PCR, although Southern blotting is still the only method to discriminate cccDNA from other DNA intermediates. In this study, we have established a robust method for untying mature rcDNA into double stranded linear DNA using specific polymerases. Untying rcDNA provides not only an alternative method for cccDNA quantification but also a sensitive method for visualizing cccDNA. We combined this method with plasmid-safe DNase and T5 exonuclease preprocessing and revealed that accurate quantification requires cccDNA digestion by a restriction enzyme because heat stability of cccDNA increases after T5 exonuclease treatment. In digital PCR using duplex TaqMan probes, fewer than 1000 copies of cccDNA were successfully visualized as double positive spots that were distinct from single positives derived from untied rcDNA. This method was further applied to the infection model of primary hepatocytes treated with nucleoside analogues and a core protein allosteric modulator to monitor cccDNA levels. Relative quantification of cccDNA by human genome copy demonstrated the possibility of precise evaluation of cccDNA level per nucleus. These results clearly indicate that the sequential reaction from untying rcDNA is useful to investigate cccDNA fates in a small fraction of nuclei.

Keywords: hepatitis B virus, cccDNA, quantification, digital PCR

51 ## Introduction

52 More than 250 million people worldwide are chronically infected with hepatitis B virus
53 (HBV), which causes about 0.9 million deaths annually [1]. Current treatment options for
54 chronic hepatitis B are limited to pegylated interferon-α (PEG-IFN) and nucleos(t)ide
55 analogues (NAs), but hepatitis B surface antigen (HBsAg) loss can only be achieved in
56 <10% of patients after PEG-IFN therapy and rarely in NA-treated patients. Even after
57 HBsAg loss, the risk of hepatocellular carcinoma persists because of the presence of
58 intrahepatic HBV DNA [2], and hepatitis B can be reactivated if the immune response of
59 the host is compromised [3]. This treatment efficacy compares unfavorably with the
60 current direct antiviral therapies for chronic hepatitis C virus, which can eradicate the
61 virus in >90% of treated patients [1, 4].

62 HBV replicates through production of daughter genomic DNA in the form of relaxed
63 circular (rc) DNA with un-ligated gaps via transcription of pregenomic RNA
64 intermediates from mature covalently closed circular (ccc) DNA [5]. A true cure for HBV
65 will require elimination of cccDNA; however, understanding of the molecular
66 mechanisms involved in the conversion of rcDNA to cccDNA and replenishment of
67 cccDNA is limited. After the identification of human sodium taurocholate co-transporting
68 peptide (NTCP) as an entry receptor for HBV [6], robust HBV infection systems have
69 become available for studying the early phases of infection. More recently, a mouse model
70 in which primary human hepatocytes (PHHs) are transplanted into urokinase-type
71 plasminogen activator-transgenic/severe combined immunodeficiency (uPA/SCID) mice
72 was introduced to support the complete HBV life cycle [7]. Although Southern blot
73 hybridization following Hirt DNA extraction is the gold standard for discriminating
74 cccDNA from rcDNA intermediates [8], cccDNA contents are too low to detect on a
75 microtiter plate, which prevents high-throughput screening [3, 9]. While real-time PCR

76 can improve sensitivity, elimination of rcDNA, which is 1000 times more abundant than
77 cccDNA and possesses an identical nucleotide sequence, is necessary for quantification
78 of cccDNA [3, 9, 10]. For decomposition limited to rcDNA, plasmid-safe ATP-dependent
79 DNase (PSAD) has been used for more than 15 years [11], but it cannot hydrolyze rcDNA
80 with a nearly complete positive strand (hereafter mature rcDNA) [3, 12]. Recently, T5
81 exonuclease (T5Exo) [9, 12] and the combination of exonuclease I and III [10] have been
82 reported to catalyze complete rcDNA degradation; however, distinguishing between
83 cccDNA and rcDNA in these reports still relies on visualization by Southern blot.
84 Herein, we have established a robust method for untying mature rcDNA into double
85 stranded linear (dsl) DNA through a DNA polymerase reaction. Untying rcDNA has been
86 developed not only as an alternative method for accurate cccDNA quantification but also
87 as a sensitive visualization tool for cccDNA by digital PCR using duplex TaqMan probes.
88 We applied these methods in practice using a liver specimen from an HBV-infected
89 humanized liver mouse [13] and an i*n vitro* culture in which HBV replication was blocked
90 by NAs and a heteroaryldihydropyrimidine (HAP)-type core protein allosteric modulator
91 (CpAM) [14]. Furthermore, relative quantification of cccDNA using human genome copy
92 number demonstrated precise evaluation of cccDNA level per nucleus in a small portion
93 of nuclei.
94
95

96 ## Methods

97 ### Plasmid clones and infected liver specimens

98 The plasmid pCR2.1DR-DR, which is a one-copy length HBV DNA clone amplified
99 by PCR from the negative strand of HBV genomic DNA [15], has 3 EcoRI recognition

100 sites on both ends of the cloning site and within the HBV genome. EcoRI-digested
101 pCR2.1DR-DR was used with an equal mixture of DR1-downstream and DR2-upstream
102 fragments of HBV DNA (DR-DR DNA). The HBV-cloned plasmid pBSadr2 [16] is a 2-
103 tandem-copy of the full-length HBV genome flanked by XhoI sites. XhoI-digested
104 pBSadr2 was used as a digested full-length HBV genome (XhoI-HBV DNA). HBV
105 infection of humanized liver mice was as described previously [13], and the liver samples
106 were stored at -80°C. The backgrounds of the mice (Table S1) and the kinetics of viral
107 and human serum albumin levels (Fig. S1) are summarized.
108

109 **Cell culture**

110 T23 cells that produced HBV genotype C (Accession# AB206816) [17] were cultured
111 in Dulbecco modified Eagle medium (DMEM, Nacalai Tesque) containing 1×antibiotic-
112 antimycotic (Nacalai Tesque), 1× nonessential amino acids (Gibco), 0.4 mg/mL
113 hygromycin B (WAKO), and 10% fetal bovine serum (FBS, Biological industries) at 37°C
114 in 5% CO_2. After confluence was reached, culture medium was changed to DMEM with
115 2% FBS without hygromycin B, and the culture was maintained for a week. Culture
116 supernatant was collected and filtered with 0.1 μm pore filter. The filtered supernatant
117 was concentrated by Amicon Ultra-15 100 kDa filter unit (Merck Millipore) and was used
118 as a source of HBV infection. PXB-cells, PHHs explanted from humanized liver mice,
119 were purchased from PhoenixBio (Hiroshima, Japan). PXB-cells were maintained in a
120 24-well plate in dHCGM containing 10% FBS and 2% dimethyl sulfoxide (DMSO) with
121 at 37°C in 5% CO_2. Infection source was mixed in dHCGM and adjusted to final 4%
122 polyethylene glycol (PEG) 6000 and overlaid on cell culture. After one day, infection
123 source was discarded, and the plate was washed twice with PBS. Infected cells were

124 cultured in dHCGM containing 10% FBS which was changed every 5 days with a one-
125 day allowance. Lamivudine was purchased from Tokyo Chemical Industry (Japan), and
126 entecavir and HAP-A (PubChem CID: 58665790) were synthesized at Mitsubishi Tanabe
127 Pharma. Drugs were dissolved in DMSO and mixed with the media to adjust to final 12.5
128 or 10 μM drugs and 2% DMSO.
129

130 **HBV DNA sample preparation**

131 T23 cells were lysed in a lysis buffer (10 mmol/L TrisHCl, pH 8.0, 1 mmol/L EDTA,
132 50 mmol/L NaCl, 8% sucrose, 0.2% NP-40) and centrifuged at 800×g for 15 min.
133 Supernatant was treated by micrococcal nuclease (New England BioLabs [NEB]) and
134 centrifuged at 20,000×g for 5 min. After core particles were precipitated with PEG6000
135 on ice for 1 h, followed by centrifugation at 20,000×g for 5 min, the precipitate was
136 digested by 0.1 mg/mL proteinase K (Wako) and 0.1% SDS at 50°C for 0.5 to 3 h, and
137 rcDNA in core particles was purified by phenol extraction and ethanol precipitation.
138 Dissected liver tissues or culture cells were homogenized in 200–500 μL of TE
139 (50:10) buffer (50 mmol/L TrisHCl, pH 7.5, 10 mmol/L EDTA) on ice. 10% SDS was
140 added to the homogenate to adjust to a final concentration of 0.5% and grinded by pestle.
141 After 3 mol/L KCl was added at final concentration 0.5 mol/L, the mixture stood at room
142 temperature for 30 min. After centrifugation for 10 min at 20,000×g, the supernatant was
143 collected, and Hirt DNA samples were purified twice by phenol extraction and ethanol
144 precipitation [8, 18]. To separate the cytoplasmic and nuclear fractions, a tissue or cell
145 culture sample was homogenized in homogenization buffer (10 mmol/L TrisHCl, pH 7.5,
146 3 mmol/L $MgCl_2$, 0.25 mol/L sucrose, 0.05% NP-40) on ice. After centrifugation at
147 10,000×g for 5 min, the supernatant was transferred to another tube and used as the

148 cytoplasmic fraction. After precipitates were washed once in homogenization buffer, the
149 resulting precipitates were used as the nuclear fraction. The number of nuclei was counted
150 after 0.5% crystal violet /0.1 M citric acid staining under a microscopic examination.
151 Using the procedure described above, Hirt DNA samples were prepared from nuclear
152 fractions, while cytoplasmic and total DNA samples were obtained after SDS-proteinase
153 K digestion.
154

155 **Enzyme reaction to HBV DNA sample**

156 To prepare a mature rcDNA control in this study, rcDNA in a core particle was treated
157 with 300 unit/mL PSAD in 1× PSAD reaction buffer (33 mmol/L Tris-acetate, pH 7.5, 66
158 mmol/L potassium acetate, 10 mmol/L magnesium acetate, 5.0 mmol/L dithiothreitol
159 [DTT]) containing 1 mmol/L ATP at 37°C for 4 h, followed by inactivation at 75°C for
160 30 min. Bst2.0 DNA polymerase (BsDP, NEB) at final 80 unit/mL reacted to DNA
161 samples in 20 μL of 1×isothermal amplification buffer (10 mmol/L $(NH_4)_2SO_4$, 50
162 mmol/L KCl, 2 mmol/L $MgSO_4$, 0.1% Tween-20, 20 mmol/L Tris-HCl, pH 8.8)
163 containing 0.7 mmol/L deoxynucleoside triphosphate at 65°C for 30 min, followed by
164 inactivation at 80°C for 20 min. Four to ten μL of this reaction mixture was further reacted
165 with PSAD in 20 μL of PSAD reaction buffer adjusting to a final Mg^{2+} concentration of
166 10 mM at 37°C for 2 to 4 h, followed by inactivation at 75°C for 30 min. For DNA
167 polymerization with other enzymes, a Taq polymerase product (ExTaq, TakaraBio), Phi29
168 DNA polymerase (NEB), and *E. coli* DNA polymerase I (Pol I, TakaraBio), were also
169 evaluated in a bundled buffer according to the manufacturer's instructions.
170 As an optimized protocol, Hirt and whole DNA samples were pretreated with 500
171 unit/mL T5 exonuclease (NEB) in 50 μL of 1×CutSmart buffer (NEB) containing 10

172 μg/mL RNase A (Nacalai Tesque), 30 units of EcoRV-HF (NEB), and 1 mmol/L DTT at
173 37 ° C for 2 h. Pretreated samples were purified by MonoFas DNA purification kit I (GL
174 Sciences Inc.), and purified DNA was eluted in 16 μL of TE buffer (10 mM Tris-HCl,
175 pH8.5, 0.5 mM EDTA). Eluted DNA was sequentially treated with 80 units/mL BsDP at
176 65° C for 30 min, followed by inactivation at 80°C for 20 min and PSAD at 37° C for 4
177 to 12 h, followed by inactivation at 75°C for 30 min, as described above. To linearize
178 cccDNA, 5 μL of the final reaction mixture was mixed with an equal volume of 0.5×
179 CutSmart buffer containing 2 u each of BamHI-HF and XhoI (NEB) and incubated at 37°
180 C for 1 h before HBV DNA quantification.
181

182 **Southern blot analysis**

183 DNA samples and DNA Molecular Weight Marker III labeled with digoxigenin (DIG)
184 (Roche Applied Science) were electrophoresed in 1.5 or 2.0% agarose gel /0.5× Tris-
185 acetate-EDTA with mobility of around 1 cm/h below 8° C. After the gel had soaked for
186 depurination in 0.25 mol/L HCl/1.5 mol/L NaCl for 10 min, denaturation in 0.5 mol/L
187 NaOH/1.5 mol/L NaCl for 30 min, and neutralization in 1 mol/L TrisHCl, pH 7.5/1.5
188 mol/L NaCl for 30 min, DNA was transferred by capillary blotting with 20×SSC onto a
189 positive-charge membrane [Biodyne Plus (PALL) or Zeta-Probe(Bio-Rad)]. The
190 transferred membrane was UV-crosslinked, dried, and stored under refrigeration. DIG
191 High Prime DNA labeling and detection starter kit II (Roche Applied Science) was used
192 for the following hybridization and detection steps. DIG-labeled HBV DNA prepared
193 from a XhoI fragment of pBSadr2 was used to probe HBV DNA. After prehybridization
194 with DIG Easy Hyb solution at 42° C for 30 min, the membrane was hybridized with
195 DIG-labeled probe at 45° C for half a day. The hybridized membrane was washed in

196 2×SSC/0.1% SDS twice for 5 to 15 min at room temperature, and in 0.5×SSC/0.1% SDS
197 twice for 15 min at 65° C. Chemiluminescence reaction was done following the
198 manufacturer's recommendation and results were read by ImageQuant LAS 4000 or 500
199 (GE Healthcare) imaging analysis.
200

201 **Quantification by real-time PCR and digital PCR**

202 DNA samples were mixed in a 10 μL reaction mixture containing 300 nmol/L TaqMan
203 probe, 200 nmol/L each of forward and reverse primers targeting the HBV S region [19]
204 (Table S2), and half the volume of the TaqMan Fast Advanced Master Mix (Life
205 technologies). They were transferred to a QuantStudio 6 Flex real-time PCR system (Life
206 technologies) for uracil-N-glycosylase treatment at 50° C for 2 min and 40 cycles of
207 denaturing step at 95° C for 1 s and extension step at 60 ° C for 20 s. Using a known
208 concentration of a linearized plasmid HBV genome, a 10× serial dilution series in
209 nuclease-free water containing 0.2 μg/μL yeast transfer RNA was prepared for calibration
210 curve analysis in each assay. To facilitate relative quantification via TaqMan copy number
211 reference assay, human RNase P and TERT (Life technologies) were also added in certain
212 multiplex assays.

213 Two TaqMan probes and primer sets located upstream of DR2 and downstream of DR1
214 were designed based on conserved regions among HBV genotypes with an equivalent
215 amplification efficiency estimated from entropy (Table S2). DNA samples were mixed in
216 the reaction mixture containing final 125 nmol/L TaqMan probe and primer sets and 1×
217 QuantStudio 3D Digital PCR Master Mix v2 (Life technologies). 14.5 μL of the mixture
218 was applied to a reaction chip, which was subsequently filled with mineral oil and sealed.
219 After PCR using a ProFlex thermal cycler (Life technologies), digital PCR results were

220 acquired by QuantStudio 3D (Life technologies) and analyzed using AnalysisSuite
221 software.
222
223

224 Results

225 Untying mature rcDNA by polymerase reaction

226 After the PSAD reaction, mature rcDNA still remained [12,20]. Since it requires a
227 circular form with about 250 bases of the annealed overhang at the 5' ends of both strands,
228 we hypothesized that extension from the 3’ ends would untie mature rcDNA into dslDNA
229 (Fig. 1A). To demonstrate this concept, BsDP was selected because of its strand
230 displacement activity. Extension product was hydrolyzed by PSAD, and HBV DNA
231 content were measured (Fig. 1B). Mature rcDNA decreased more than 2 log-fold after
232 extension with BsDP at 80 unit/mL followed by PSAD treatment. In the repeated
233 experiment, BsDP-PSAD treatment again achieved more than 2 log-fold degradation of
234 mature rcDNA, while undigested plasmids were unchanged (Fig. 1C). The structural
235 change of mature rcDNA was analyzed by Southern blot hybridization (Fig. 1D). Mature
236 rcDNA was observed as 4.5-kb band and was shifted to 3.5-kb after BsDP reaction,
237 consistent with stable dslDNA that is 250 bases longer than single-copy length HBV,
238 while PSAD alone did not affect. The band disappeared after the sequential reaction of
239 BsDP and PSAD. Therefore, we concluded that BsDP extension converts mature rcDNA
240 into stable dslDNA that is susceptible to PSAD. We additionally checked whether other
241 polymerases with either strand displacement or 5' to 3' exonuclease activities could untie
242 mature rcDNA (Fig. S2). ExTaq was evaluated with or without initial heat denaturing at
243 98°C for 1 min. While heat denaturing made rcDNA susceptible to PSAD, similar results

244 were obtained in BsDP and ExTaq treatments without heat denaturing. However, Phi29
245 DNA polymerase and Pol I, with a lower optimum temperature, did not alter susceptibility
246 to PSAD.
247

248 **Application to accurate cccDNA quantification**

249 In Hirt DNA samples from HBV-infected cells, both cccDNA as well as deproteinized
250 rcDNA are present during Southern blot analysis [17]. Since conventional PSAD and
251 recently T5Exo are used to eliminate rcDNA, we intended to check compatibility of this
252 untying method after these preprocessing methods. HBV DNA levels after preprocessing
253 with PSAD and T5Exo were compared in T23, an HBV-producing cell line. Cytoplasmic
254 DNA and Hirt DNA from whole cell and nuclear fractions were prepared and dissolved
255 at 6.8×10^4 cells equivalent per μL in which HBV DNA levels were 7.4, 6.5, and 4.8 log10
256 copies/μL, respectively. Column-purified DNA samples after nuclease preprocessing 1)
257 were sequentially reacted with 2) BsDP, 3) PSAD, and 4) BamHI and XhoI restriction
258 enzymes (RE) that cut HBV DNA, and HBV DNA levels at 1) to 4) were determined. We
259 performed two independent assays and merged the results (Fig. 2A). T5Exo at ≥ 0.1
260 unit/μL decomposed to a greater extent than PSAD. While quantitative values did not
261 change after the BsDP reaction, those after PSAD decreased 1–2 log-fold. Of note,
262 quantitative values after RE digestion increased about 1 log-fold in the plasmid controls
263 and Hirt DNAs preprocessed with T5Exo at 0.4 unit/μL. Although T5Exo at 0.4 unit/μL
264 and higher seemed to hydrolyze more rcDNA and contaminated genomic DNA in whole
265 Hirt DNA, we could obtain almost the same levels of HBV DNA in nuclear Hirt DNA
266 after applying the subsequent reactions.
267 To confirm the robustness of this method in an infected humanized mouse liver [13],

268 we picked 3 small pieces out of each liver from 6 mice (Table S1) from which cytoplasmic
269 DNA and nuclear Hirt DNA samples had been prepared. Subsequent enzyme reactions
270 were performed in 2 independent batches. As a reaction control, cytoplasmic core rcDNA
271 from T23 decreased 4 log-fold by preprocessing with 0.5 unit/μL T5Exo, and additionally
272 1 log-fold decomposition was achieved after the subsequent reactions (Fig. 2B). Accurate
273 results were obtained from 2 independent assays, and the difference between cytoplasmic
274 DNA and cccDNA were less than 3 log-fold (Fig. 2C). Therefore, 5 log-fold
275 decomposition of cytoplasmic core rcDNA in the control reactions meant less than 1% of
276 cccDNA and is sufficient for accurate cccDNA quantification. The averages of the
277 quantified values from 3 small pieces from the same liver are shown with serum HBV
278 DNA (Fig. 2D).
279

280 **Discrimination between cccDNA and rcDNA by digital PCR using duplex**
281 **probes**

282 As a visualization method to confirm cccDNA purity, we developed a method to
283 discriminate between cccDNA and untied rcDNA by digital PCR using duplex probes
284 (Fig. 3A). After RE digestion away from the DR2-DR1 region, dslDNA from untied
285 rcDNA changes into two fragments containing either DR2-upstream or DR1-downstream,
286 while cccDNA changes into a single fragment containing both. When duplex TaqMan
287 probes are designed upstream of DR2 and downstream of DR1, these fragments can be
288 distinguished as single and double positive spots in microcells of digital PCR. The
289 quantification principle of digital PCR is based on the Poisson distribution [21], that is, a
290 random variable X which takes a natural number where $\lambda > 0$ satisfies $P(X = k) =$
291 $\frac{\lambda^k e^{-\lambda}}{k!}$. Specifically, the logarithmic probability of negative spots, $-lnP(0)$, yields λ

292 copy/spot as a measured value, and the probability of positive spots therefore becomes
293 $1 - P(0)$, namely $1 - e^{-\lambda}$. Because the probability of pseudo double positive spots that
294 contain both single-positive fragments increases in proportion to dslDNA, we
295 mathematically estimated an optimal range to discriminate cccDNA in a mixture. When
296 a specimen contains untied rcDNA only, the probabilities of double and single positive
297 spots are $\left(1 - e^{-\lambda}\right)^2$ and $e^{-\lambda}\left(1 - e^{-\lambda}\right)$, respectively, and the simulation suggests that
298 total copies in an assay should not exceed 5,000 to maintain a rate of <30% pseudo double
299 positives (Fig. S3). With this limitation, we also calculated the frequency of single and
300 double positive spots from the rc/ccc mixture at different ratios (Fig. 3B). The estimated
301 numbers of single and double positive spots competed with 40% cccDNA specimen, and
302 double positive spots are apparently dominant when cccDNA exceeds half.

303 This method was assessed using a model genome of untied rcDNA and cccDNA, DR-
304 DR DNA and XhoI HBV DNA, respectively. We designed two TaqMan probes based on
305 conserved regions shared among genotypes A to H (Table S2) and optimized the reaction
306 conditions to achieve equivalent amplification efficiency (Fig. 3C). Reaction mixtures
307 containing 2-fold dilution series of DR-DR DNA or XhoI-HBV DNA were processed in
308 a microcell chip where the spots were scanned (Fig. 3D). Almost the same copy numbers
309 were reported from both channels in all samples; therefore, the reaction condition is
310 optimal. The ratios of double positive spots in the actual measurements generally agreed
311 with those from the Poisson model simulation (Table 1). Moreover, purity of cccDNA
312 was also evaluated in the authentic samples from Fig. 2C. These samples were further
313 digested by HincII to cut between DR2 and DR1, and Southern blot analysis confirmed
314 that double-positive fragment from cccDNA was cleaved into two single-positive
315 fragments (Fig. 4AB). The same samples for accurate cccDNA quantification were
316 successfully visualized by digital PCR (Fig. 4C) to confirm cccDNA purity (Table S3).

317

318 **Use for drug evaluation in cell culture system and cccDNA level per cell**

319 Accurate cccDNA quantification developed in this study was applied to an i*n vitro*
320 study. After an inoculum prepared from T23 culture supernatant was infected into PXB-
321 cells, HBV production in the supernatant continued for more than 40 days in a manner
322 dependent on the infection dose, and the intracellular HBV contents also correlated with
323 infection dose even after long-term culture (Fig. 5AB). When viral replication was
324 stopped at the time of infection by treatment with entecavir, lamivudine, and HAP-A at
325 12.5 μmol/L, HBV DNA levels in supernatant continued to decline in the drug-treated
326 groups, and cytosolic HBV DNA levels per well decreased from 5×10^5 in DMSO control
327 to 10^4 in the drug-treated groups (Fig. 5CD). However, nuclear cccDNA levels per well
328 were almost the same at around 10^4 in the control and NA-groups, while that in the HAP-
329 A was below the limit of quantification (Fig. 5D).

330 To determine the cccDNA level per cell using human genome copy number, PXB-cells
331 were infected with HBV at multiplicities of infection of 100 and 300 genome equivalents
332 with or without 10 μmol/L HAP-A. After 9 and 14 days, whole cell lysate was prepared
333 and divided equally into two portions, after which one was centrifuged to fractionate
334 cytosolic supernatant and nuclear precipitate. DNA samples were prepared by SDS-
335 proteinase K digestion and Hirt extraction from whole lysate and cytosolic supernatant.
336 After removal of nuclei, cccDNA contents in Hirt DNA became undetectable, while
337 changes in total HBV DNA levels were minimal (Fig. 6A). Therefore, the remaining
338 nuclear faction contained most of the cccDNA, and it was used to determine relative
339 cccDNA quantification per nucleus. The nuclear suspension was dispensed to 3 or 4 wells
340 in a microtiter plate at 100 to 1000 nuclei per well and treated with proteinase K, in which

341 the quantification cycle (C_q) value for the internal standard (IS) was determined using
342 human RNaseP and TERT probes. Remaining samples were preprocessed by PSAD and
343 further treated to eliminate mature rcDNA, and HBV C_q values were determined. Mean
344 $\Delta C_q(HBV - IS)$ values are shown in bars (Fig. 6B), and relative amounts of HAP-A to
345 control calculated by $2^{\Delta\Delta Cq}$ indicated that drug efficacy on cccDNA establishment can
346 be evaluated in a small portion of infected nuclei. In order to assess the influence of
347 altering the DNA preparation method, nuclear fractions were prepared from the same liver
348 specimens. A portion of the total DNA that was extracted from 5×10^5 nuclei by the SDS-
349 proteinase K method was treated for accurate cccDNA quantification. HBV DNA levels
350 were determined absolutely based on the standard curve method with nuclear count
351 normalization (Fig. 6C), and relative amounts were calculated from compensated
352 $\Delta C_q(IS - HBV)$ (Fig. 6D).
353
354

355 **Discussion**

356 Although hydrolysis of rcDNA intermediates by PSAD has already been adopted,
357 rcDNA with a nearly complete positive strand still remains problematic [12, 20]. While
358 heat denaturing is an option to distinguish rcDNA and cccDNA [22], elimination of
359 denatured products is required for PCR assay. Complete rcDNA decomposition methods
360 using T5Exo [9, 12] and exonuclease I and III combination [10] have been introduced;
361 however, the use of these nucleases is controversial in practice [23]. In contrast to
362 hydrolysis by nucleases, our approach is based on structural changes in the mature rcDNA
363 by polymerase reaction, namely untying rcDNA (Fig. 1A), and BsDP is suitable for this
364 purpose (Fig. 1B-D).

365 Interestingly, only BsDP and Taq polymerase could catalyze the untying reaction,
366 whereas Phi29 DNA polymerase, which catalyzes rolling cycle amplification, and Pol I,
367 which is used for nick translation, could not. These results indicate the importance of
368 reaction temperature and/or activity on the 5'-DNA and RNA flaps of mature rcDNA (Fig.
369 S2). We chose BsDP for the other parts of this study because it can be inactivated by heat
370 to enable a one-tube reaction.

371 We next demonstrated the combination of the untying method with preprocessing by
372 PSAD and T5Exo for accurate cccDNA quantification in HBV producing cells and the
373 human-chimeric mouse liver samples (Fig. 2) because cccDNA contents in the equivalent
374 mouse model had previously been determined in total DNA hydrolyzed by PSAD [23-
375 25]. Although a previous study indicated that reaction conditions with T5Exo should be
376 restricted because of a significant degradation of control plasmid [9], PSAD and T5Exo
377 degraded control plasmid around 1-log fold in this study (Fig 1C and Fig 2A). A certain
378 amount of nicked plasmid that was from an alkaline-lysis preparation may be a substrate
379 for the sequential treatment (Fig 1C). However, no difference among the preprocessing
380 conditions was observed even using a relatively higher concentration and longer reaction
381 time (Fig 2A). Instead, PCR amplification was less effective in the cccDNA samples after
382 preprocessing with T5Exo in a dose-dependent manner (Fig. 2A). Therefore, we argue
383 that T5Exo treatment stabilizes cccDNA and prevents accurate quantification without
384 linearization. Since variance among dissections from the same liver was much smaller
385 than variance among individuals (Fig. 2CD), we assume that cccDNA is accurately
386 quantified by this method. Whereas the hepatocellularity of the human liver is roughly
387 10^5 per mg [26], cccDNA level per cell is discussed later.

388 Besides improved elimination of rcDNA, discrimination between rcDNA and cccDNA
389 relies on the difference between C_q values from over-gap PCR [3, 9, 10]. In this study,

390 digital PCR using duplex probes has been applied to visualize cccDNA purity in low copy
391 samples (Fig. 3). While several studies utilized digital PCR for cccDNA quantification,
392 cccDNA-specific detection had not been achieved [27-30]. Furthermore, over-gap PCR
393 is difficult to adapt to an end-point assay like digital PCR because the threshold to
394 distinguish pseudo-positives from rcDNA is unclear. The sequential reaction from
395 untying mature rcDNA makes the samples ready for charging into the microcells, and the
396 thermal profile is fixed for duplex PCR (Fig. 3AB). As the experimental data corresponds
397 reasonably well with the simulated values (Table 1) as well as the successful visualization
398 of authentic cccDNA samples (Fig. 4), we concluded that cccDNA is purified sufficiently
399 after the sequential reaction developed in this study.

400 The PXB-cell system was introduced as a highly reproducible model for HBV infection
401 [7]; however, inoculum preparation from culture supernatants had been limited to the cell
402 lines of genotype D [31-33]. Since the major genotype in the Asia-Pacific region is
403 genotype C [34], the inoculum in this study was prepared from culture supernatant of T23,
404 a genotype C-producing cell line [17, 35]. While a significant increase in cccDNA level
405 was reported around 40 days post-infection in HepG2-NTCP-K7 cells [36], cccDNA
406 levels in PXB-cells 35 days after infection were not different between NA-treated and
407 control groups (Fig. 5D). This result indicates that HBV infection spreads poorly in non-
408 dividing cell culture. Excellent work with serially transplanting infected PHH into naïve
409 uPA/SCID/beige mice revealed that non-proliferating human hepatocytes served as a viral
410 reservoir [23]; therefore, destabilizing cccDNA in PXB-cells may lead to curative
411 therapies for chronic hepatitis B. Contrary to NAs, HAP-A at high dose hindered cccDNA
412 formation as several CpAMs did in the previous reports [37-39]. A recent study shows
413 that another HAP derivative destabilizes and diminishes incoming capsids during *de novo*
414 HBV infection [40].

415 Although quantifying cellular DNA is equally important in quantifying the cccDNA
416 level per cell, host genomic DNA is discarded during Hirt DNA preparation. After
417 verifying that cccDNA was undetectable in the cytosolic fraction (Fig. 6A), we evaluated
418 cccDNA levels normalized by host genome copy number in a small portion of nuclear
419 suspensions (Fig. 6B). Although a previous study employed single nucleus assay in duck
420 hepatitis B virus (DHBV) infection [41], ours began with 100–1000 nuclei because the
421 mean cccDNA level is lower than in DHBV and about one tenth dilution from the initial
422 suspension is unavoidable for cccDNA purification. Consequently, relative changes in
423 cccDNA level by $\Delta\Delta C_q$ was possible even in a small fraction of nuclei. After the
424 $\Delta C_q(IS - HBV)$ value was compensated for the gap between HBV standard curve and
425 C_q of IS from known nuclear count, cccDNA levels from $2^{\Delta Cq}$ ranged between 0.01–1 per
426 nucleus, which agreed very well with those of absolute quantification (Fig. 6CD).
427 Therefore, we assume that compensation for ΔC_q contributes to accurate transformation
428 into cccDNA level per nucleus.

429 As a reservoir for persistence, accurate quantification of cccDNA is important for viral
430 kinetics modeling [42, 43] and warrants investigation of therapeutic interventions to cure
431 chronic hepatitis B [44-46]. The sequential reactions initiated from untying rcDNA
432 remedies a defect in PSAD alone, and optimization for a single tube reaction makes
433 accurate cccDNA quantification convenient. Moreover, visual discrimination between
434 cccDNA and rcDNA in digital PCR becomes possible in the same specimens with less
435 than 1000 copies. This method will be applicable for discriminating other structurally
436 different forms along with proper exonucleases and REs. The latest study proposes
437 essential components for cccDNA formation, but this work has been done using a model
438 genome [47]. Naturally, this machinery should be verified in natural infection; thus, the
439 method described here can be conductive to illustrating intranuclear intermediates that

440 were not visible before.

441

442 ## Conflicts of interest

443 Naohiro Kamiya, Takahiko Sugimoto, Yasunori Tsuboi, and Akira Mogami are
444 employees of Mitsubishi Tanabe Pharma Corporation. The others declare that there are
445 no conflicts of interest relating this work.

446

447 ## Funding information

448 K. C. received the research grant related to hepatitis B from the Japan Agency for
449 Medical Research and Development, AMED (grant number, 20fk0310109h0004). The
450 funder had no role in study design, data collection and analysis, decision to publish or
451 preparation of the manuscript. No other external funding was received for this study.

452

453 ## Acknowledgement

454 We thank Tesuaki Ishikawa, Kyoko Yamasaki, and Shigeki Hoshino for their supports
455 and constructive discussions.

456

457 ## Ethical approval

458 All procedures performed in this study involving animals were in accordance with the
459 guidelines and approved by Hiroshima University Animal Research Committee, and all
460 animals received humane care.

461

462

463 **References**

464 1. Ward JW, Hinman AR. What is needed to eliminate hepatitis B virus and hepatitis
465 C virus as global health threats. *Gastroenterology* 2019;156:297–310. doi:
466 10.1053/j.gastro.2018.10.048.
467 2. Terrault NA, Lok ASF, McMahon BJ, Chang K-M, Hwang JP, Jonas MM, *et al*.
468 Update on prevention, diagnosis, and treatment of chronic hepatitis B: AASLD
469 2018 Hepatitis B Guidance. *Hepatology* 2018;67:1560–1599. doi:
470 10.1002/hep.29800.
471 3. Nassal M. HBV cccDNA: viral persistence reservoir and key obstacle for a cure
472 of chronic hepatitis B. *Gut* 2015;64:1972–1984. doi: 10.1136/gutjnl-2015-
473 309809.
474 4. Hu J, Protzer U, Siddiqui A. Revisiting hepatitis B virus: challenges of curative
475 therapies. *J Virol* 2019;93:e01032–19. doi: 10.1128/JVI.01032-19.
476 5. Seeger C, Mason WS. Molecular biology of hepatitis B virus infection. *Virology*
477 2015;479-480:672–686. doi: 10.1016/j.virol.2015.02.031.
478 6. Yan H, Zhong G, Xu G, He W, Jing Z, Gao Z, *et al.* Sodium taurocholate
479 cotransporting polypeptide is a functional receptor for human hepatitis B and D
480 virus. *Elife* 2012;1:e00049. doi: 10.7554/eLife.00049.
481 7. Ishida Y, Yamasaki C, Yanagi A, Yoshizane Y, Fujikawa K, Watashi K, *et al*.
482 Novel robust in vitro hepatitis B virus infection model using fresh human
483 hepatocytes isolated from humanized mice. *Am J Pathol* 2015;185:1275–1285.
484 doi: 10.1016/j.ajpath.2015.01.028.
485 8. Cai D, Nie H, Yan R, Guo JT, Block TM, Guo H. A southern blot assay for
486 detection of hepatitis B virus covalently closed circular DNA from cell cultures.
487 *Methods Mol Biol* 2013;1030:151‑161. doi: 10.1007/978-1-62703-484-5_13.

488 9. Qu B, Ni Y, Lempp FA, Vondran FWR, Urban S. T5 exonuclease hydrolysis of
489 hepatitis B virus replicative intermediates allows reliable quantification and
490 fast drug efficacy testing of covalently closed circular DNA by PCR. *J Virol*
491 2018;92:e01117-18. doi: 10.1128/JVI.01117-18.
492 10. Luo J, Cui X, Gao L, Hu J. Identification of an intermediate in hepatitis B virus
493 covalently closed circular (CCC) DNA formation and sensitive and selective
494 CCC DNA detection. *J Virol* 2017;91:e00539-17. doi: 10.1128/JVI.00539-17.
495 11. Werle-Lapostolle B, Bowden S, Locarnini S, Wursthorn K, Petersen J, Lau G, *et*
496 *al.* Persistence of cccDNA during the natural history of chronic hepatitis B and
497 decline during adefovir dipivoxil therapy. *Gastroenterology* 2004;126:1750–
498 1758. doi: 10.1053/j.gastro.2004.03.018.
499 12. Zhang X, Lu W, Zheng Y, Wang W, Bai L, Chen L, *et al*. In situ analysis of
500 intrahepatic virological events in chronic hepatitis B virus infection. *J Clin Invest*
501 2016;126:1079–1092. doi: 10.1172/JCI83339.
502 13. Uchida T, Imamura M, Kan H, Hiraga N, Hayes CN, Tsuge M, *et al*.
503 Usefulness of humanized cDNA-uPA/SCID mice for the study of hepatitis B
504 virus and hepatitis C virus virology. *J Gen Virol* 2017;98:1040–1047. doi:
505 10.1099/jgv.0.000726.
506 14. Deres K, Schröder CH, Paessens A, Goldmann S, Hacker HJ, Weber O, *et al*.
507 Inhibition of hepatitis B virus replication by drug-induced depletion of
508 nucleocapsids. *Science* 2003;299:893–896. doi: 10.1126/science.1077215.
509 15. Günther S, Li BC, Miska S, Krüger EH, Meisel H, Will H. A novel method for
510 efficient amplification of whole hepatitis B virus genomes permits rapid
511 functional analysis and reveals deletion Mutants in immunosuppressed patients.
512 *J Virol* 1995;69:5437–5444. doi: 10.1128/JVI.69.9.5437-5444.1995.

513 16. Tsurimoto T, Fujiyama A, Matsubara K. Stable expression and replication of
514 hepatitis B virus genome in an integrated state in a human hepatoma cell line
515 transfected with the cloned viral DNA. *Proc Natl Acad Sci USA* 1987;84: 444–
516 448. doi: 10.1073/pnas.84.2.444.
517 17. Hayes CN, Akamatsu S, Tsuge M, Miki D, Akiyama R, Abe H, *et al.* Hepatitis
518 B virus-specific miRNAs and Argonaute2 play a role in the viral life cycle.
519 *PLoS ONE* 2012;7:e47490.
520 18. Guo H, Jiang D, Zhou T, Cuconati A, Block TM, Guo JT. Characterization of the
521 intracellular deproteinized relaxed circular DNA of hepatitis B virus: an
522 intermediate of covalently closed circular DNA formation. *J Virol*
523 2007;81:12472–12484. doi: 10.1128/JVI.01123-07.
524 19. Liu Y, Hussain M, Wong S, Fung SK, Yim HJ, Lok ASF. A genotype-independent
525 real-time PCR assay for quantification of hepatitis B virus DNA. *J Clin*
526 *Microbiol*. 2007;45: 553–558. doi: 10.1128/JCM.00709-06.
527 20. Köck J, Rösler C, Zhang J-J, Blum HE, Nassal M, Thoma C. Generation of
528 covalently closed circular DNA of hepatitis B viruses via intracellular recycling
529 is regulated in a virus specific manner. *PLoS Pathog* 2010;6:e1001082. doi:
530 10.1371/journal.ppat.1001082.
531 21. Majumdar N, Banerjee S, Pallas M, Wessel T, Hegerich P. Poisson plus
532 quantification for digital PCR systems. *Sci Rep* 2017;7:9617. doi:
533 10.1038/s41598-017-09183-4.
534 22. Tang L, Sheraz M, McGrane M, Chang J, Guo JT. DNA polymerase alpha is
535 essential for intracellular amplification of hepatitis B virus covalently closed
536 circular DNA. *PLoS Pathog* 2019;15:e1007742. doi:
537 10.1371/journal.ppat.1007742.

538 23. Allweiss L, Volz T, Giersch K, Kah J, Raffa G, Petersen J, *et al.* Proliferation of
539 primary human hepatocytes and prevention of hepatitis B virus reinfection
540 efficiently deplete nuclear cccDNA in vivo. *Gut* 2018;67:542–552. doi:
541 10.1136/gutjnl-2016-312162.
542 24. Volz T, Allweiss L, MBarek MB, Warlich M, Lohse AW, Pollok JM, *et al*. The
543 entry inhibitor Myrcludex-B efficiently blocks intrahepatic virus spreading in
544 humanized mice previously infected with hepatitis B virus. *J Hepatol*
545 2013;58:861–867. doi: 10.1016/j.jhep.2012.12.008.
546 25. Klumpp K, Shimada T, Allweiss L, Volz T, Lütgehetmann M, Hartman G, *et al.*
547 Efficacy of NVR 3-778, alone and in combination with pegylated interferon, vs
548 entecavir in uPA/SCID mice with humanized livers and HBV infection.
549 *Gastroenterology* 2018;154:652–662. doi: 10.1053/j.gastro.2017.10.017.
550 26. Wilson ZE, Rostami-Hodjegan A, Burn JL, Tooley A, Boyle J, Ellis SW, *et al.*
551 Inter-individual variability in levels of human microsomal protein and
552 hepatocellularity per gram of liver. *Br J Clin Pharmacol.* 2003;56:433–440. doi:
553 10.1046/j.1365-2125.2003.01881.x.
554 27. Mu D, Yan L, Tang H, Liao Y. A sensitive and accurate quantification method
555 for the detection of hepatitis B virus covalently closed circular DNA by the
556 application of a droplet digital polymerase chain reaction amplification system.
557 *Biotechnol Lett* 2015;37:2063–73. doi: 10.1007/s10529-015-1890-5.
558 28. Caviglia GP, Abate ML, Tandoi F, Ciancio A, Amoroso A, Salizzoni M, *et al.*
559 Quantitation of HBV cccDNA in anti-HBc-positive liver donors by droplet
560 digital PCR: A new tool to detect occult infection. *J Hepatol* 2018;69:301–307.
561 doi: 10.1016/j.jhep.2018.03.021.
562 29. Huang JT, Yang Y, Hu YM, Liu XH, Liao MY, Morgan R, *et al*. A highly sensitive

563 and robust method for hepatitis B virus covalently closed circular DNA detection
564 in single cells and serum. *J Mol Diagn* 2018;20:334–343. doi:
565 10.1016/j.jmoldx.2018.01.010.
566 30. Bao CY, Hung HC, Chen YW, Fanb CY, Huang CJ, Huang W. Requirement of
567 cyclin-dependent kinase function for hepatitis B virus cccDNA synthesis as
568 measured by digital PCR. Ann Hepatol 2020;19:280–286. doi:
569 10.1016/j.aohep.2019.12.005.
570 31. Nakabori T, Hikita H, Murai K, Nozaki Y, Kai Y, Makino Y, *et al*. Sodium
571 taurocholate cotransporting polypeptide inhibition efficiently blocks hepatitis B
572 virus spread in mice with a humanized liver. *Sci Rep* 2016;6:27782. doi:
573 10.1038/srep27782.
574 32. Kitamura K, Que L, Shimadu M, Koura M, Ishihara Y, Wakae K, *et al*. Flap
575 endonuclease 1 is involved in cccDNA formation in the hepatitis B virus. *PLoS*
576 *Pathog* 2018;14:e1007124. doi: 10.1371/journal.ppat.1007124.
577 33. Luo J, Xi J, Gao L, Hu J. Role of hepatitis B virus capsid phosphorylation in
578 nucleocapsid disassembly and covalently closed circular DNA formation. *PLoS*
579 *Pathog* 2020;16:e1008459. doi: 10.1371/journal.ppat.1008459.
580 34. Velkov S, Ott JJ, Protzer U, Michler T. The global hepatitis B virus genotype
581 distribution approximated from available genotyping data. *Genes (Basel)*
582 2018;9:495. doi: 10.3390/genes9100495.
583 35. Makokha GN, Abe-Chayama H, Chowdhury S, Hayes CN, Tsuge M, Yoshima T,
584 *et al*. Regulation of the Hepatitis B virus replication and gene expression by the
585 multi-functional protein TARDBP. *Sci Rep* 2019;9:8462. doi: 10.1038/s41598-
586 019-44934-5.
587 36. Ko C, Chakraborty A, Chou WM, Hasreiter J, Wettengel JM, Stadler D, *et al.*

588 Hepatitis B virus genome recycling and de novo secondary infection events
589 maintain stable cccDNA levels. *J Hepatol* 2018;69:1231–1241. doi:
590 10.1016/j.jhep.2018.08.012.
591 37. Berke JM, Dehertogh P, Vergauwen K, Van Damme E, Mostmans W, Vandyck
592 K, *et al.* Capsid assembly modulators have a dual mechanism of action in
593 primary human hepatocytes infected with hepatitis B virus. *Antimicrob Agents*
594 *Chemother* 2017;61:e00560-17. doi: 10.1128/AAC.00560-17.
595 38. Guo F, Zhao Q, Sheraz M, Cheng J, Qi Y, Su Q, *et al.* HBV core protein allosteric
596 modulators differentially alter cccDNA biosynthesis from de novo infection and
597 intracellular amplification pathways. *PLoS Pathog* 2017;13:e1006658. doi:
598 10.1371/journal.ppat.1006658.
599 39. Lahlali T, Berke JM, Vergauwen K, Foca A, Vandyck K, Pauwels F, *et al*. Novel
600 potent capsid assembly modulators regulate multiple steps of the hepatitis B
601 virus life cycle. *Antimicrob Agents Chemother* 2018;62:e00835-18. doi:
602 10.1128/AAC.00835-18.
603 40. Ko C, Bester R, Zhou X, Xu Z, Blossey C, Sacherl J, *et al.* A new role for capsid
604 assembly modulators to target mature hepatitis B virus capsids and prevent virus
605 infection. *Antimicrob Agents Chemother* 2019;64:e01440-19. doi:
606 10.1128/AAC.01440-19.
607 41. Zhang YY, Zhang BH, Theele D, Litwin S, Toll E, Summers J. Single-cell
608 analysis of covalently closed circular DNA copy numbers in a hepadnavirus-
609 infected liver. *Proc Natl Acad Sci USA* 2003;100:12372–12377. doi:
610 10.1073/pnas.2033898100.
611 42. Ishida Y, Chung TL, Imamura M, Hiraga N, Sen S, Yokomichi H, *et al*. Acute
612 hepatitis B virus infection in humanized chimeric mice has multiphasic viral

613 kinetics. *Hepatology* 2018;68:473‑484. doi: 10.1002/hep.29891.
614 43. Goyal A, Liao LE, Perelson AS. Within-host mathematical models of hepatitis B
615 virus infection: past, present, and future. *Curr Opin Syst Biol* 2019;18:27‑35.
616 doi: 10.1016/j.coisb.2019.10.003.
617 44. Mu D, Yuan FC, Chen Y, Jiang XY, Yan L, Jiang LY, *et al*. Baseline value of
618 intrahepatic HBV DNA over cccDNA predicts patient's response to interferon
619 therapy. *Sci Rep* 2017;7:5937. doi: 10.1038/s41598-017-05242-y.
620 45. Hong X, Kim ES, Guo H. Epigenetic regulation of hepatitis B virus covalently
621 closed circular DNA: Implications for epigenetic therapy against chronic
622 hepatitis B. *Hepatology* 2017;66:2066-2077. doi: 10.1002/hep.29479
623 46. Testoni B, Lebosse F, Scholtes C, Berby F, Miaglia C, Subic M, *et al.* Serum
624 hepatitis B core-related antigen (HBcrAg) correlates with covalently closed
625 circular DNA transcriptional activity in chronic hepatitis B patients. *J Hepatol*
626 2019;70:615‑625. doi: 10.1016/j.jhep.2018.11.030.
627 47. Wei L, Plos A. Core components of DNA lagging strand synthesis machinery are
628 essential for hepatitis B virus cccDNA formation. *Nat Microbiol* 2020;5:715–
629 726. doi: 10.1038/s41564-020-0678-0.
630

631 **Tables**

632

633 Table 1. Total- and double-positive spots in actual assay using model genome of

634 dsl and cccDNA by digital PCR using duplex probes.

Sample	Dilution	Channel	Measurements					Poisson model (rc only)		
			Total copies	Qualified spots	Total pos.	Double pos.	% of Double	Total pos.	Double pos	% of Double
rc mimic	0	FAM	12036.0	15312	7130	3434	48.2	8335	4537	54.4
DR-DR		VIC	11953.9	15312	7095	3434	48.4	8298	4497	54.2
EcoRI	-1	FAM	6150.2	17674	4843	1363	28.1	5194	1526	29.4
		VIC	6136.7	17674	4834	1363	28.2	5185	1521	29.3
	-2	FAM	3154.9	17658	2675	384	14.4	2889	473	16.4
		VIC	3064.1	17658	2604	384	14.7	2813	448	15.9
	-3	FAM	1538.6	17380	1338	124	9.3	1472	125	8.5
		VIC	1527.7	17380	1329	124	9.3	1463	123	8.4
ccc mimic	0	FAM	5101.8	14034	3274	3112	95.1	4277	1304	30.5
XhoI HBV		VIC	4961.3	14034	3195	3111	97.4	4179	1245	29.8
	-1	FAM	3229.4	17606	2725	2653	97.4	2951	494	16.8
		VIC	3206.2	17606	2707	2651	97.9	2931	488	16.6
	-2	FAM	1449.7	17811	1295	1244	96.1	1392	109	7.8
		VIC	1473.1	17811	1315	1244	94.6	1414	112	7.9
	-3	FAM	696.8	15968	569	548	96.3	682	29	4.3
		VIC	695.6	15968	568	548	96.5	681	29	4.3

635

636

637

638 **Fig. legends**

639

640 Fig. 1 Untying rcDNA by DNA polymerase reaction

641 (A) Schematic drawing of linearization of relaxed-circular (rc)DNA to double strand
642 linear (dsl)DNA by DNA extension using a polymerase with strand displacement activity.
643 DR1 and DR2 represent direct repeat regions in the HBV genome. (B) Titration of Bst2.0
644 DNA polymerase (BsDP) for untying rcDNA was performed with various Mg^{2+}
645 concentrations on 9 log copies of mature rcDNA control and dslDNA mimic, DR-DR
646 DNA, equivalent to 10 log copies in 20 μL. One fifth of these reaction mixtures were
647 treated with Plasmid-safe ATP-dependent DNase (PSAD) in 20 μL in which HBV DNA
648 concentration was measured. (C) Extension with BsDP was repeated using 9 log copies
649 of mature rcDNA and circular plasmid controls, pCR2.1DR-DR and pBSadr2. (D)
650 Southern blot analysis of DNA fragments derived from mature rcDNA after treatment
651 with BsDP and PSAD. M: DNA Molecular Weight Marker III, DIG-labeled (Roche), 1-
652 cp: 1 copy. (E) Other polymerases were tested for untying mature rcDNA followed by
653 decomposition by PSAD. Before extension by ExTaq, the template was treated with (+)
654 or without (-) heating to 98˚C for 1 min. Reaction temperature and polymerase
655 concentration were adapted to manufacturer instructions.

656

657 Fig. 2 Application of untying rcDNA method to accurate cccDNA quantification

658 (A) HBV DNA levels at each sequential reaction (1–4) were monitored in the
659 fractionates from T23 HBV-producing cells. DNA samples from the cytoplasmic fraction
660 were prepared by SDS-proteinase K treatment. Hirt DNA samples were prepared from
661 whole cell (WC) and nuclear fractions. Each fraction contained 3.4×10^6 cells. Controls
662 were prepared from 10^9 copies of HBV-cloned plasmid, pCR2.1DR-DR, with and without

663 digestion by EcoRI. All DNA samples were dissolved in 50 μL of Tris-EDTA after phenol
664 extraction and ethanol precipitation. Before nuclease treatment, HBV DNA levels in
665 cytoplasmic, WC, and nuclear fractions were 7.4, 6.5, and 4.8 log10 copies/μL,
666 respectively, while that in the control was 7.2 log10 copies/μL. Ten μL of these DNA
667 samples were hydrolyzed by PSAD or T5Exo in 50 μL of a reaction mixture with RNase
668 A and EcoRV, which do not cut HBV, and were purified using a silica column. 1)
669 Preprocessed DNA was treated sequentially by 2) BsDP extension, 3) PSAD
670 decomposition, and 4) digestion by BamHI and Xho I to cut cccDNA as described in the
671 Methods. Two experiments were performed independently and merged in these panels.
672 (B–D) HBV DNA content in infected liver samples from six mice were evaluated with a
673 control reaction. To assess reproducibility, this assay was conducted in two independent
674 batches according to the optimized condition described in the Methods. (B) HBV DNA
675 levels at each sequential reactions in control DNAs like A. (C) Three small pieces (#1-3)
676 from each liver (7.8–31 mg) were homogenized separately and cytoplasmic DNA and
677 nuclear Hirt DNA were prepared. One-fifth volume of Hirt DNA was treated in the
678 sequential reaction with controls to eliminate rcDNA. HBV DNA levels in both fractions
679 were determined. (D) Summarization of the quantified values by an individual mouse
680 with background information. Means with standard errors of cytosolic and nuclear
681 cccDNA levels were calculated.

682

683 Fig. 3 Discrimination between cccDNA and rcDNA by digital PCR using duplex
684 probes

685 (A) Schematic drawing of discrimination between untied rcDNA and cccDNA using
686 duplex probes. In microcells, cccDNA is always detected as a double positive spot, while
687 rcDNA is detected as single positive spots with a high probability. (B) Simulated number
688 of single and double positive spots to be observed in digital PCR in a rc/ccc mixed

689 samples. The number of spots theoretically follows the Poisson distribution; therefore,
690 the total number of qualified spots is fixed to 15,000, and the proportion of cccDNA in a
691 mixture is set to 0.2, 0.4, and 0.6 in each panel. (C) Amplification plot of TaqMan probe-
692 primer sets designed for this assay. Designed primer and probe sets located on DR2
693 upstream (1551YB) and DR1 downstream (1874FB) are summarized in Table S2. The
694 dilution series of HBV DNA standard was amplified using these sets separately or mixed
695 in real-time PCR. Quantification cycles (C_q) in each color are plotted. (D) Actual assay
696 using model genome of rc and cccDNA. The serial 2-fold dilution was prepared from
697 0.04 pg of DR-DR DNA and 0.02 pg of XhoI-HBV DNA. The X- and Y axes represent
698 the FAM and VIC channels of the duplex probes, respectively, and the reported copy
699 numbers in total from each channel by QuantStudio 3D AnalysisSuite software are
700 indicated in the upper-right corner. The numbers of total- and double-positive spots are
701 summarized in Table 1.
702
703 Fig. 4 Visualizing authentic cccDNA prepared in this study
704 (A) Schematic of confirmation of cccDNA purity in samples prepared for accurate
705 cccDNA quantification. After linearization by XhoI and BamHI, the samples are
706 additionally digested by HincII to alter double positive to single positives. The sizes of
707 fragments from genotype C are indicated. (B) Actual visualization of cccDNA from an
708 infected liver by Southern blot. Purified cccDNA and pBSadr2 (0.1 ng) were digested and
709 loaded in 2% agarose gel. Filled and open arrows indicate double- and single- positive
710 fragments, respectively. M: DNA Molecular Weight Marker III, DIG-labeled (Roche). (C)
711 The samples that were identical to Fig. 2C were diluted to 500–2000 copies per assay to
712 visualize cccDNA content adequately. The reported copy number in total from each
713 channel by QuantStudio 3D AnalysisSuite software and the numbers of total- and double-

714 positive spots are summarized in Table S3.

715

716 Fig. 5 Evaluation of establishment of cccDNA pool in the PXB cell culture
717 system

718 (A, B) PXB-cells, PHHs expanded in uPA/SCID mice, were infected by positive
719 control mouse serum containing 4×10^6 copies/mL HBV genotype C and a dilution series
720 of inoculum that was concentrated to 10-fold from nearly 10^9 copies/mL culture
721 supernatant of T23, an HBV genotype C-producing cell line (N=2). Mean viral loads in
722 culture supernatants during more than 40 days of culture (A) and means with SD of
723 cytosolic DNA and nuclear cccDNA in harvested cells (B) are shown. (C, D) PXB cells
724 were again infected by one tenth dilution of the same inoculum. At the time of infection,
725 12.5 μmol/L drug treatments were initiated to block viral replication completely (N=3).
726 Means with standard errors of viral loads in the supernatant (C) as well as cytosolic DNA
727 and nuclear cccDNA in harvested cells (D) are shown. LLOQ: lower limit of
728 quantification.

729

730 Fig. 6 Relative quantification of cccDNA to an internal standard of genomic
731 DNA

732 (A, B) PXB-cells were infected using concentrated T23 supernatant at the indicated
733 multiplicity of infection (MOI), and treatment with 10 μmol/L HAP-A was initiated at the
734 same time. The cells were harvested at 9 and 14 days after infection and were lysed to
735 fractionate the cytosol and nucleus (N=2). (A) Total DNA and cccDNA samples were
736 prepared from whole lysate and the excluded nuclei fraction. Mean HBV DNA levels are
737 shown as bars. The percent of DMSO control in cccDNA from whole cells is indicated
738 above the bars. (B) Nuclear suspension was dispensed to 3 or 4 wells of a reaction plate
739 for each and were digested by SDS-proteinase K where C_q values of both IS were

740 determined. The remaining samples were further treated to purify cccDNA where HBV
741 C_q values were determined. After a maximum of 40 cycles is set, as summarized in Table
742 S4, the mean ΔC_q values with SD were determined. Relative cccDNA levels in HAP-A
743 vs DMSO by $2^{\Delta\Delta Cq}$ are shown above the bars. Asterisks indicate that HBV negatives were
744 included. (C, D) Nuclear samples were prepared from two sections of each of the same
745 livers as evaluated in Fig. 2C. Total DNA was extracted from 5×10^5 nuclei by SDS-
746 proteinase K treatment and was digested by HindIII and EcoRV. A portion of the digested
747 DNA was treated to purify cccDNA, and total DNA and cccDNA were quantified by real-
748 time PCR using HBV and each of RNaseP and TERT probes. (C) HBV DNA levels were
749 determined by a standard curve and were normalized by a nuclear count. The mean and
750 SD of two assays is shown. (D) Relative HBV DNA copies per nucleus are shown with
751 SD. ΔC_q(HBV-IS)* indicates mean ΔC_q values based on RNaseP and TERT to
752 compensate for the gap between the HBV standard curve and the C_q of IS from the known
753 nuclear count.

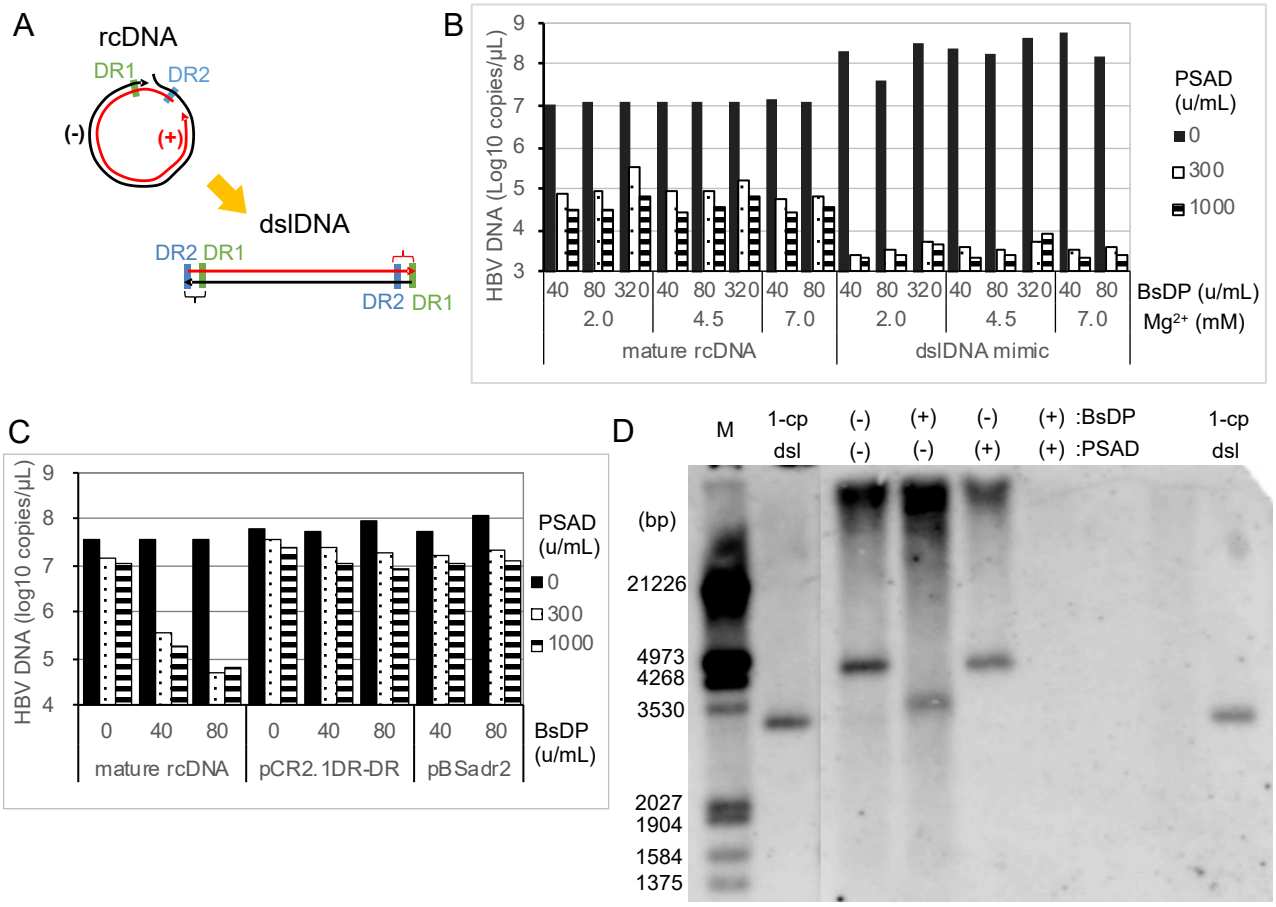
A
rcDNA
DR1
DR2
(-)
(+)
dslDNA
DR2 DR1
DR2 DR1
B
HBV DNA (Log10 copies/μL)
9
8
7
6
5
4
3
PSAD (u/mL)
0
300
1000
40 80 320 40 80 320 40 80 40 80 320 40 80 320 40 80
BsDP (u/mL)
2.0 4.5 7.0 2.0 4.5 7.0
Mg2+ (mM)
mature rcDNA
dslDNA mimic
C
HBV DNA (log10 copies/μL)
9
8
7
6
5
4
PSAD (u/mL)
0
300
1000
0 40 80 0 40 80 40 80
BsDP (u/mL)
mature rcDNA
pCR2.1DR-DR
pBSadr2
D
M
1-cp dsl
(-) (-)
(+) (-)
(-) (+)
(+) (+)
:BsDP
:PSAD
1-cp dsl
(bp)
21226
4973
4268
3530
2027
1904
1584
1375

Fig. 1

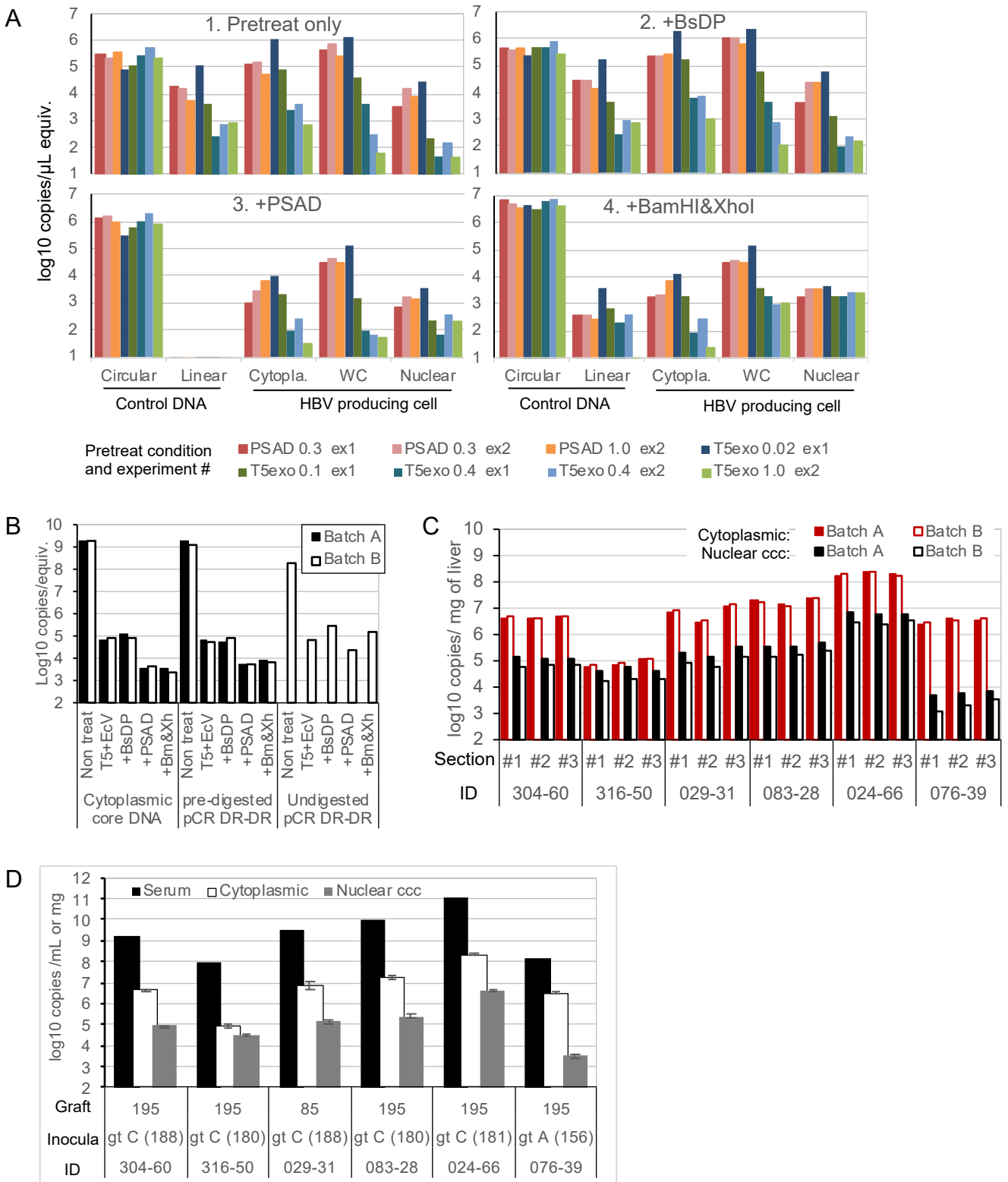
A
1. Pretreat only
2. +BsDP
3. +PSAD
4. +BamHI&XhoI
log10 copies/µL equiv.
Circular
Linear
Cytopla.
WC
Nuclear
Control DNA
HBV producing cell
Pretreat condition and experiment #
PSAD 0.3 ex1
PSAD 0.3 ex2
PSAD 1.0 ex2
T5exo 0.02 ex1
T5exo 0.1 ex1
T5exo 0.4 ex1
T5exo 0.4 ex2
T5exo 1.0 ex2
B
Log10 copies/equiv.
Batch A
Batch B
Non treat
T5+EcV
+BsDP
+PSAD
+Bm&Xh
Cytoplasmic core DNA
pre-digested pCR DR-DR
Undigested pCR DR-DR
C
log10 copies/ mg of liver
Cytoplasmic:
Nuclear ccc:
Section
ID
304-60
316-50
029-31
083-28
024-66
076-39
D
Serum
Cytoplasmic
Nuclear ccc
log10 copies /mL or mg
Graft
Inocula
ID
195
85
gt C (188)
gt C (180)
gt C (181)
gt A (156)

Fig. 2

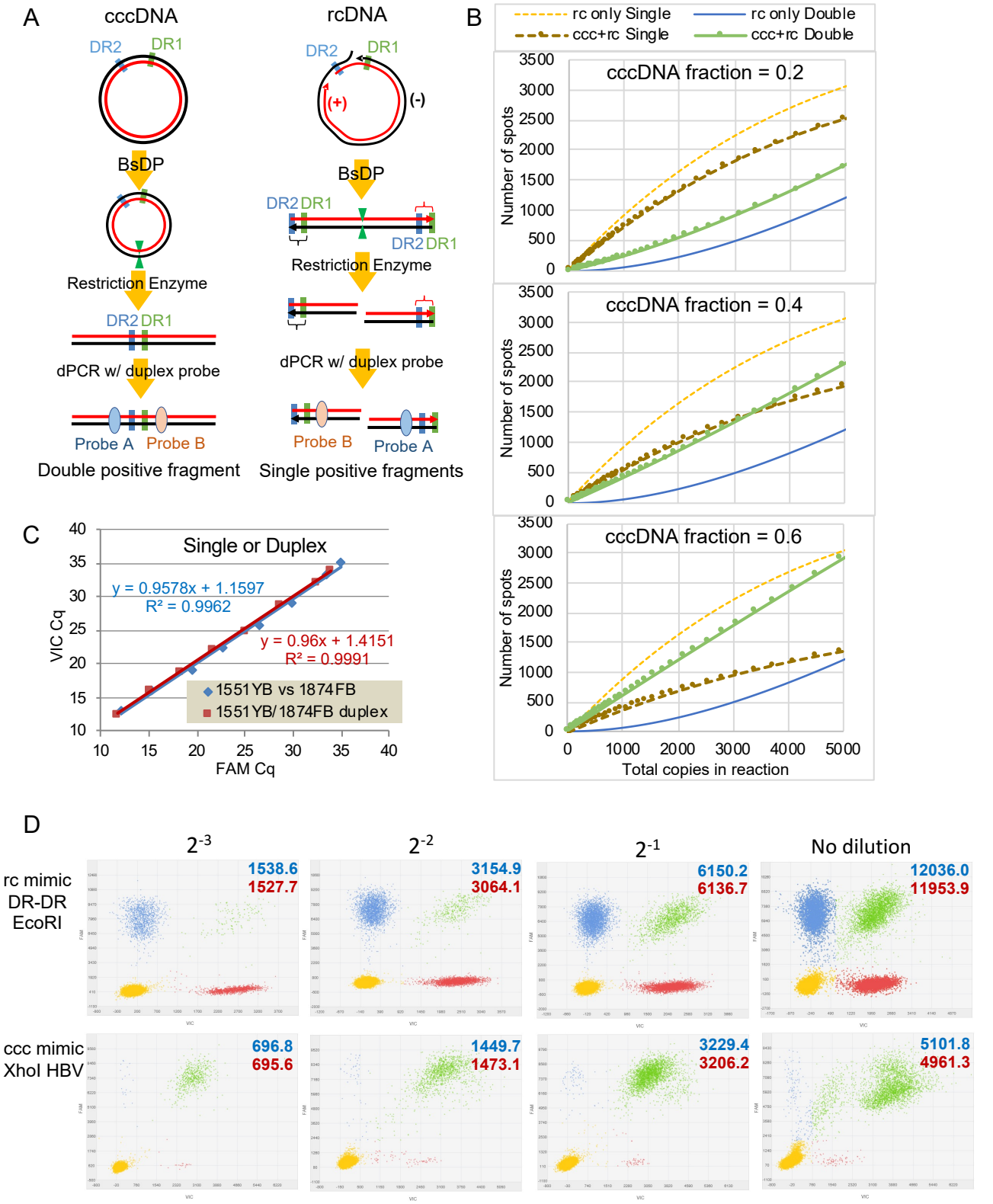
A
cccDNA
rcDNA
DR2
DR1
(+)
(-)
BsDP
Restriction Enzyme
dPCR w/ duplex probe
Probe A
Probe B
Double positive fragment
Single positive fragments
B
rc only Single
rc only Double
ccc+rc Single
ccc+rc Double
cccDNA fraction = 0.2
cccDNA fraction = 0.4
cccDNA fraction = 0.6
Number of spots
Total copies in reaction
C
Single or Duplex
y = 0.9578x + 1.1597
R² = 0.9962
y = 0.96x + 1.4151
R² = 0.9991
1551YB vs 1874FB
1551YB/1874FB duplex
VIC Cq
FAM Cq
D
2-3
2-2
2-1
No dilution
rc mimic
DR-DR
EcoRI
ccc mimic
XhoI HBV
1538.6
1527.7
3154.9
3064.1
6150.2
6136.7
12036.0
11953.9
696.8
695.6
1449.7
1473.1
3229.4
3206.2
5101.8
4961.3

Fig. 3

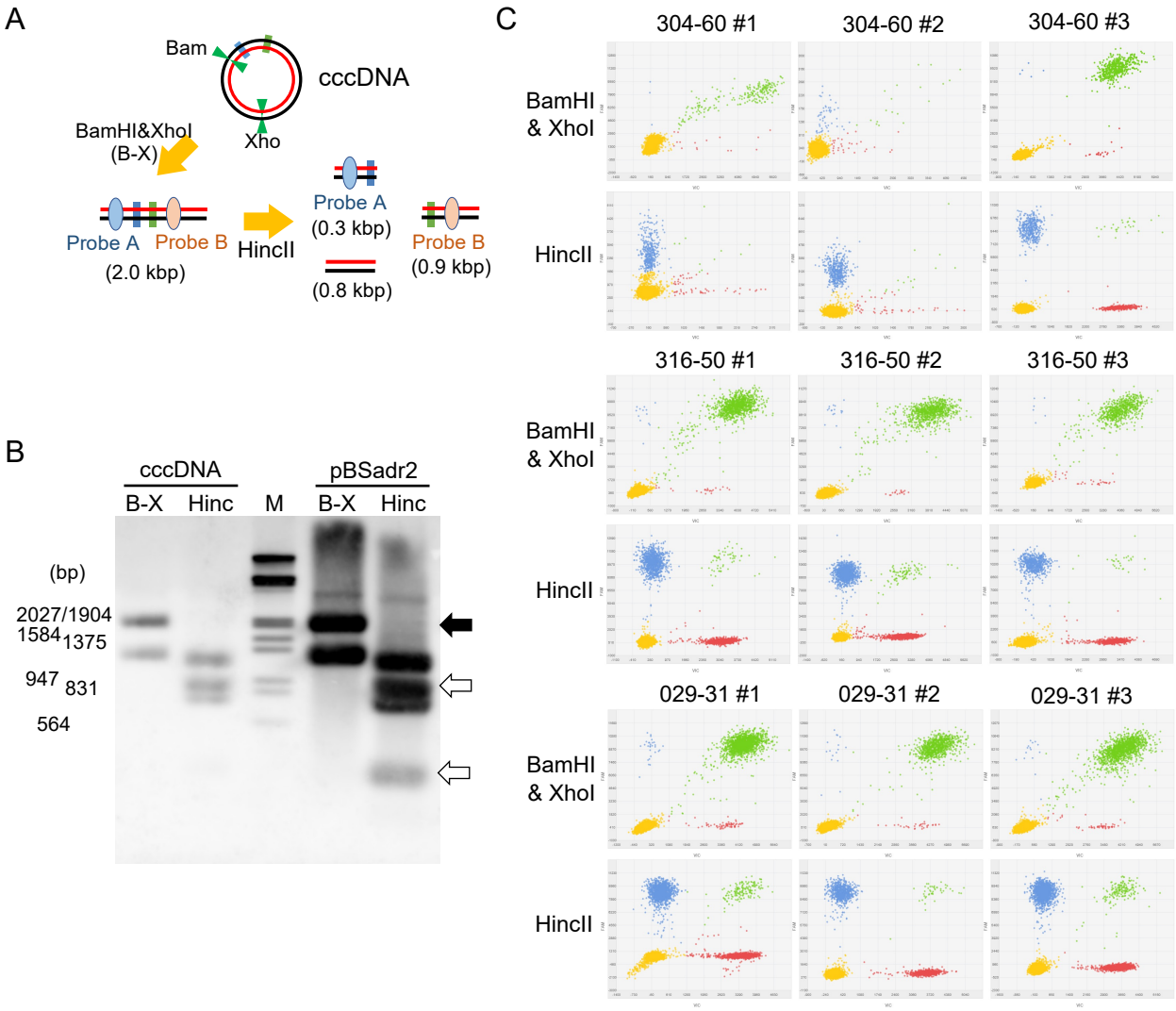
A
Bam
cccDNA
Xho
BamHI&XhoI
(B-X)
Probe A
Probe B
(2.0 kbp)
HincII
Probe A
(0.3 kbp)
(0.8 kbp)
Probe B
(0.9 kbp)
B
cccDNA
pBSadr2
B-X
Hinc
M
B-X
Hinc
(bp)
2027/1904
1584
1375
947
831
564
C
304-60 #1
304-60 #2
304-60 #3
BamHI
& XhoI
HincII
316-50 #1
316-50 #2
316-50 #3
BamHI
& XhoI
HincII
029-31 #1
029-31 #2
029-31 #3
BamHI
& XhoI
HincII

Fig. 4

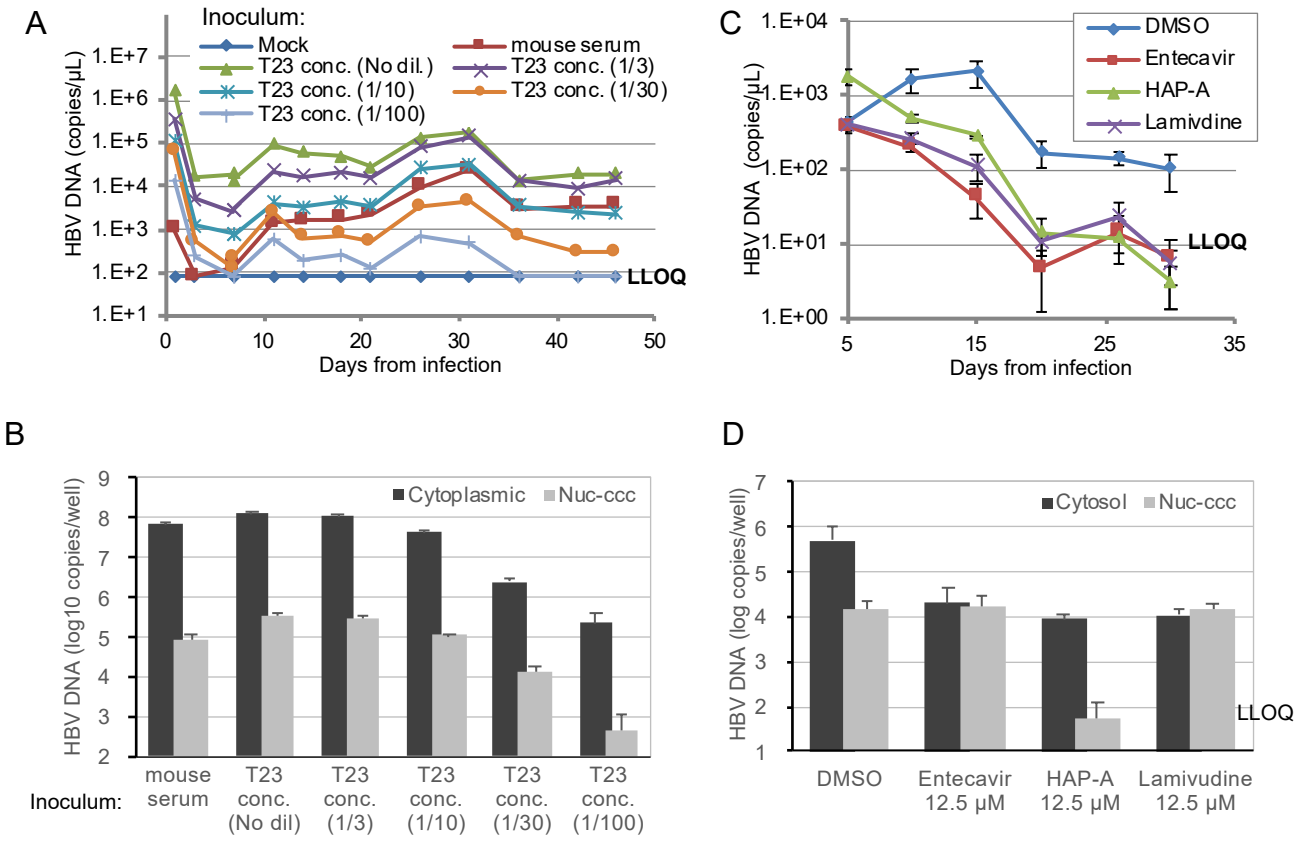
A
Inoculum:
Mock
mouse serum
T23 conc. (No dil.)
T23 conc. (1/3)
T23 conc. (1/10)
T23 conc. (1/30)
T23 conc. (1/100)
HBV DNA (copies/μL)
1.E+7
1.E+6
1.E+5
1.E+4
1.E+3
1.E+2
1.E+1
LLOQ
0
10
20
30
40
50
Days from infection
C
DMSO
Entecavir
HAP-A
Lamivdine
HBV DNA (copies/μL)
1.E+04
1.E+03
1.E+02
1.E+01
1.E+00
LLOQ
5
15
25
35
Days from infection
B
Cytoplasmic
Nuc-ccc
HBV DNA (log10 copies/well)
9
8
7
6
5
4
3
2
Inoculum:
mouse serum
T23 conc. (No dil)
T23 conc. (1/3)
T23 conc. (1/10)
T23 conc. (1/30)
T23 conc. (1/100)
D
Cytosol
Nuc-ccc
HBV DNA (log copies/well)
7
6
5
4
3
2
1
LLOQ
DMSO
Entecavir 12.5 μM
HAP-A 12.5 μM
Lamivudine 12.5 μM

Fig.5

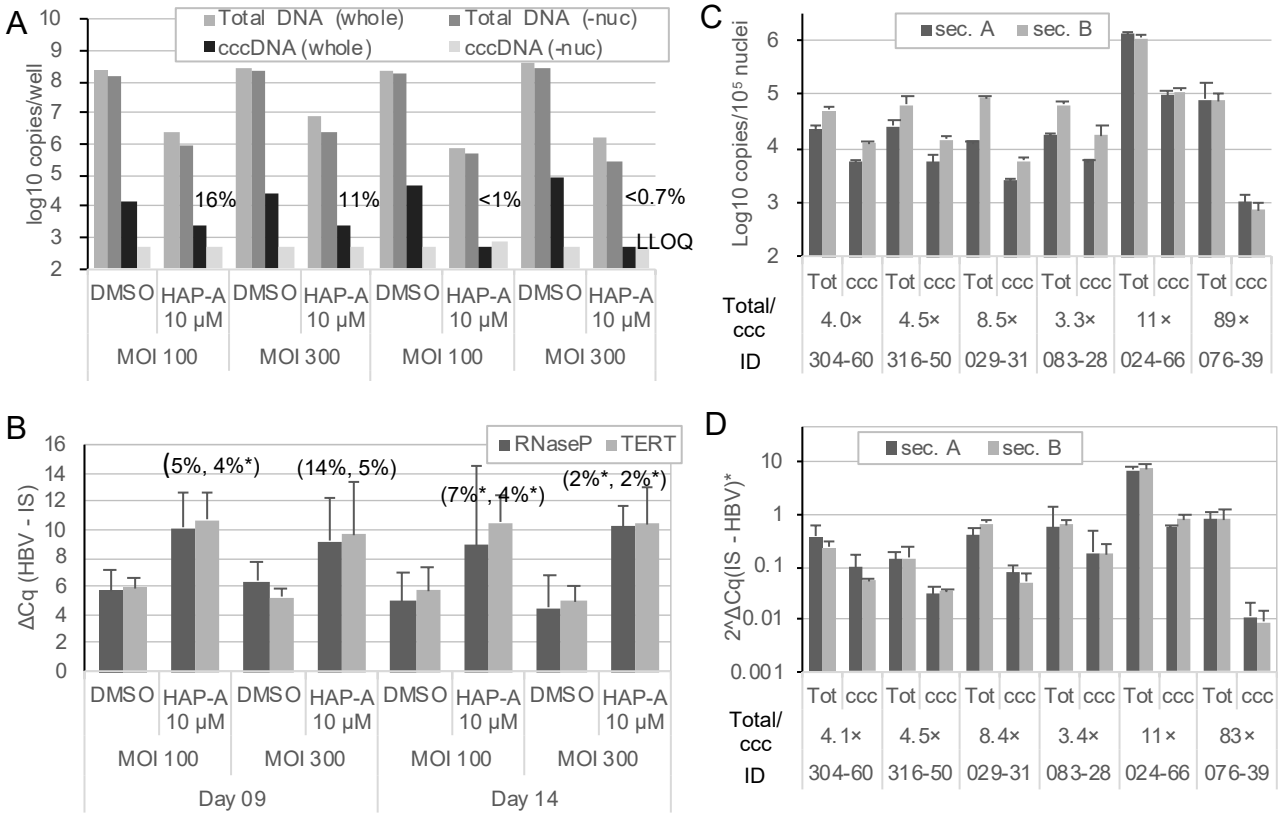
A
Total DNA (whole)
Total DNA (-nuc)
cccDNA (whole)
cccDNA (-nuc)
log10 copies/well
16%
11%
<1%
<0.7%
LLOQ
DMSO
HAP-A 10 µM
MOI 100
MOI 300
B
RNaseP
TERT
ΔCq (HBV - IS)
(5%, 4%*)
(14%, 5%)
(7%*, 4%*)
(2%*, 2%*)
Day 09
Day 14
C
sec. A
sec. B
Log10 copies/10⁵ nuclei
Tot
ccc
Total/ ccc
4.0×
4.5×
8.5×
3.3×
11×
89×
ID
304-60
316-50
029-31
083-28
024-66
076-39
D
2^ΔCq(IS - HBV)*
4.1×
4.5×
8.4×
3.4×
11×
83×

Fig. 6